

Level density calculations and the relative
yields of $^{209}\text{Bi}(\gamma, xn)$ nuclear reactions

(JINR INTEREST report)

Rade Smolović

December 2023

Abstract

The analysis of relative yields of photonuclear reactions, such as $^{209}\text{Bi}(\gamma, \text{xn})$, requires a proper theoretical prediction of cross-sections. One of the main ingredients for such cross-section calculations is the level density. Parameterizing the microscopically calculated level density onto a Fermi gas expression and using TALYS code for nuclear reactions, the cross-sections for $^{209}\text{Bi}(\gamma, \text{xn})$ reactions were obtained. These cross-sections were then used together with GEANT4 simulations of photon flux to evaluate the relative yields to be compared with the experimental ones.

Contents

1	Level density calculations	3
1.1	BCS pairing interaction	3
1.2	Grand partition function	4
1.3	Calculations	6
1.4	Parametrization	7
2	TALYS cross-section calculations	9
3	Comparison with the experiment	11
3.1	Experimental relative yields	11
3.2	Theoretical relative yields	12
3.3	Comparison and conclusions	13

Chapter 1

Level density calculations

To obtain the nuclear level density for ^{209}Bi and the daughter nuclei resulting from $^{209}\text{Bi}(\gamma, \text{xn})$, the BCS model is used to include the pairing interaction and the statistical grand partition function is used as the method of 'counting'. The obtained level density $\rho(t)$, where t is the statistical temperature, $\beta = 1/t$, is then fitted onto the Fermi gas expression $\rho(U)$, by the means of excitation energy of the quasi-particles from the BCS formalism, U , and the level density parameter $a(U)$.

1.1 BCS pairing interaction

The Hamiltonian that describes the monopole pairing interaction, $\langle v\bar{v}|V|v_1\bar{v}_1\rangle = -G$, is expressed via second quantization creation and annihilation operators $a_{k\pm}^\dagger$ and $a_{k\pm}$ as [1, 7]:

$$\hat{H} = \sum_k \varepsilon_k \left(a_{k+}^\dagger a_{k+} + a_{k-}^\dagger a_{k-} \right) - G \sum_{kk'} a_{k'+}^\dagger a_{k'-}^\dagger a_{k-} a_{k+}. \quad (1.1)$$

This way, the pairing interaction is included in the calculations by the right term in (1.1), where G is the pairing strength, while the left term corresponds to the non-interacting fermion system, and thus ε_k is the single-particle eigenenergy. The BCS model accounts for pairing interaction, and the single particle eigenenergies ε_k are taken from some standard microscopic models, such as the Nilsson model.

By the means of Bogoliubov transformations:

$$\begin{aligned}\alpha_k &= u_k a_k^\dagger - v_k a_{\bar{k}}, \\ \alpha_{\bar{k}} &= u_k a_{\bar{k}}^\dagger - v_k a_k,\end{aligned}$$

where α_k and $\alpha_{\bar{k}}$ are now the annihilation operators of the quasi-particles, and k and \bar{k} are time-reversed states such that we consider $k > 0$ only, the augmented Hamiltonian $\hat{H} - \lambda \hat{N}$ can be rearranged into different terms of α_k and $\alpha_{\bar{k}}$, such that the term describing ground-state energy is[3, 8]:

$$H_0 = \sum_k (\varepsilon_k - \lambda - E_k) + \frac{\Delta^2}{G} + \sum_{k>0} E_k \alpha_k^\dagger \alpha_{\bar{k}}, \quad (1.2)$$

which is, unlike 1.1, diagonalized. The E_k in (1.4) represents the quasi-particle excitation energies:

$$E_k = \sqrt{(\varepsilon_k - \lambda)^2 + \Delta^2}, \quad (1.3)$$

and λ is the chemical potential, and Δ is the pairing gap, which describes the pairing effect on the excitation energy. Varying augmented Hamiltonian with respect to u_k , $\delta \langle \text{BCS} | \hat{H} - \lambda \hat{N} | \text{BCS} \rangle = 0$, where $|\text{BCS}\rangle$ is the ground state, the so-called gap equation can be obtained[3, 7]:

$$\frac{2}{G} = \sum_k \frac{\tanh \frac{1}{2} \beta E_k}{E_k}. \quad (1.4)$$

1.2 Grand partition function

There are two popular methods of counting up the possible states from single-particle states: combinatorial and grand partition function methods[4]. The statistical sum is obtained using (1.2):

$$Z = \text{Tr} e^{-\beta H_0}, \quad (1.5)$$

and the grand partition function method is proceeded with. The logarithm of the grand partition function is:

$$\ln Z = -\beta \sum_k (\varepsilon_k - \lambda - E_k) + 2 \sum_k (1 + e^{-\beta E_k} - \beta \frac{\Delta^2}{G}), \quad (1.6)$$

and the system entropy is:

$$S = \ln Z + \beta E - \mu_n N - \mu_p Z. \quad (1.7)$$

The state density ρ can be found to be the inverse Laplace transform of the continuous approximation of the grand partition function integrated over the saddle points[4]:

$$\rho = \frac{e^S}{(2\pi)^{\frac{3}{2}} \sqrt{\det \left| \frac{\partial^2 S}{\partial \mu_i \partial \mu_j} \right|_{\mu_0}}}, \quad (1.8)$$

where $\det \left| \frac{\partial^2 S}{\partial \mu_i \partial \mu_j} \right|_{\mu_0}$ is the Hessian matrix of the entropy S at the saddle point. The saddle point conditions give[4]:

$$\frac{-\partial \ln Z}{\partial \beta} = E, \quad \frac{\partial \ln Z}{\partial \mu_n} = N, \quad \frac{\partial \ln Z}{\partial \mu_p} = Z, \quad (1.9)$$

these relations in combination with the gap equation (1.4) and (1.6) result in:

$$E = \sum_k \varepsilon_k \left(1 - \frac{\varepsilon - \lambda}{E_k} \tanh \frac{1}{2} \beta E_k \right) - \frac{\Delta^2}{G}, \quad (1.10)$$

$$N = \sum_k \varepsilon_k \left(1 - \frac{\varepsilon - \lambda}{E_k} \tanh \frac{1}{2} \beta E_k \right), \quad (1.11)$$

$$S = 2 \sum_k \ln(1 + e^{-\beta E_k}) + 2\beta \sum_k \frac{E_k}{1 + e^{\beta E_k}}. \quad (1.12)$$

1.3 Calculations

A Python script was made, taking as the input the considered isotope of bismuth, single-particle eigenenergies for protons and neutrons at the considered temperatures, and the binding energy of the considered and adjacent isotopes. The script produces the temperature dependence of the pairing gap, for the system of protons and neutrons separately Δ_p and Δ_n , entropy S , excitation energy $U = E - E_0$, and most importantly the level density ρ .

The level density ρ is obtained from (1.8) by knowing the entropy S , for each value of $\beta = 1/t$. The entropy S is obtained for each value of $\beta = 1/t$ by the relation (1.12), which requires the knowledge of the quasi-particle excitation E_k in (1.3).

Firstly, the gap equation (1.4) and (1.11) can be combined into a system with the unknowns G and λ . With the knowledge of Δ_0 (pairing gap at very low temperature) from the binding energy of the isotope and its neighbors, which can be obtained from some standard reference, G and λ_0 can be obtained. The obtained G is used again in these two equations to get Δ and λ for each $\beta = 1/t$ value. This calculation is carried out for protons and neutrons separately since entropy and energy are additive quantities, and so we will obtain λ_p, Δ_p for protons, λ_n, Δ_n for neutrons. We can see in Figure 1.1, for ^{207}Bi case, how Δ_p depends on the temperature t , and the critical temperature for each nucleon type, where the pairing effects disappear, can be noticed.

With the knowledge of Δ and λ , E_k can be obtained, and entropy $S = S_p + S_n$, where S_n is the entropy of the neutrons and S_p is the entropy of the protons, can be evaluated along with the Hessian matrix of the entropy, which finally results in the level density ρ , shown in the second and the third graphs in Figure 1.1.

Lastly, the excitation energy $U = E_k - E_0$ is obtained by subtracting the quasi-particle energy from the quasi-particle energy obtained using Δ_0 and λ_0 .

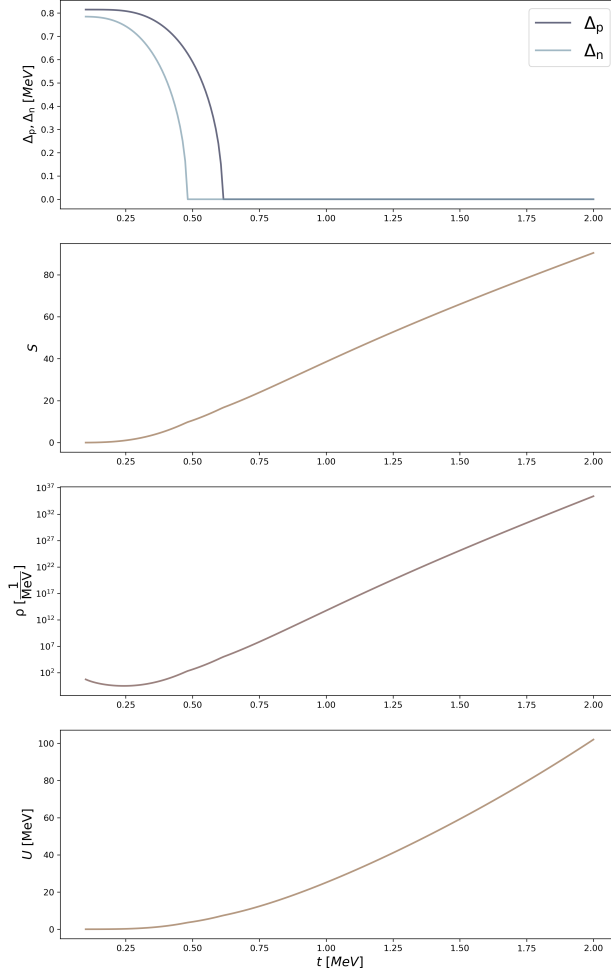


Figure 1.1: The neutron and proton pairing gaps Δ_p and Δ_n , entropy S , level density ρ , and the total excitation energy U depending on the statistical temperature t , obtained by the calculation method outlined above for ^{207}Bi isotope.

1.4 Parametrization

The Fermi Gas expression[6]:

$$\rho_{Fg} = \frac{\sqrt{\pi}}{12a^{1/4}U^{5/4}} e^{2\sqrt{aU}}, \quad (1.13)$$

is useful in the way it relates the level density to the excitation energy directly. The known ρ and U from the level density calculations above are used to obtain $a(U)$.

The obtained $a(U)$ is fitted onto the phenomenological expression[6]:

$$a(A, U) = \tilde{a}(A) \left[1 + \frac{1 - e^{-\gamma U}}{U} \delta E_{shell} \right], \quad (1.14)$$

Where γ and \tilde{a} are the damping parameter and saturation level density (reached after some U value), and δE_{shell} is the shell correction. Such calculations of level density parameter are shown for ^{203}Bi in Figure 1.2.

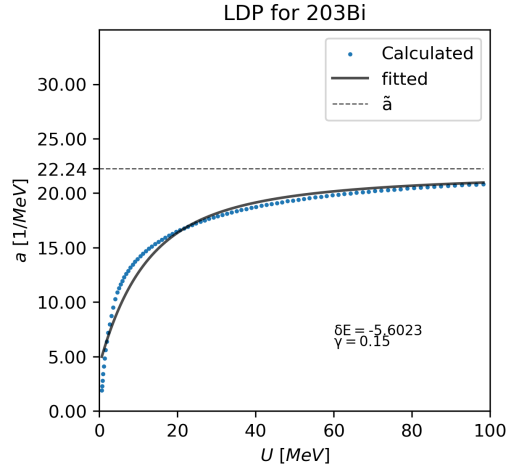


Figure 1.2: Dependence of level density parameter a on the excitation energy obtained for ^{203}Bi from the calculation methods outlined above.

Chapter 2

TALYS cross-section calculations

The code for simulating nuclear reactions, TALYS[5], is used with the level densities calculated above to obtain the cross-sections needed for evaluating the relative yields of $^{209}\text{Bi}(\gamma, \text{xn})$. To do so, the three parameters \tilde{a} , γ , and δE_{shell} , from the above calculations for ^{209}Bi and products $^{200-208}\text{Bi}$, are given as the keywords in the TALYS input for the generalized superfluid model grand partition function level density fitted onto Fermi Gas expression (ld3 model in TALYS). The results of such calculations are shown in Figure 2.1.

Using "asys y" keyword in TALYS is important for these calculations since TALYS default keyword is set to be "asys n" which means that TALYS fits the parameters \tilde{a} , γ , and δE_{shell} such that they fit with some experimental database. Another thing to consider is the use of "ejectiles n" keyword. The keyword reduces the event space, excluding for example the proton emission, thus increasing the overall probability calculations for all neutron emissions. The keyword is used to decrease the computation time, as many effects can occur after ^{209}Bi is irradiated by bremsstrahlung radiation of 100 MeV.

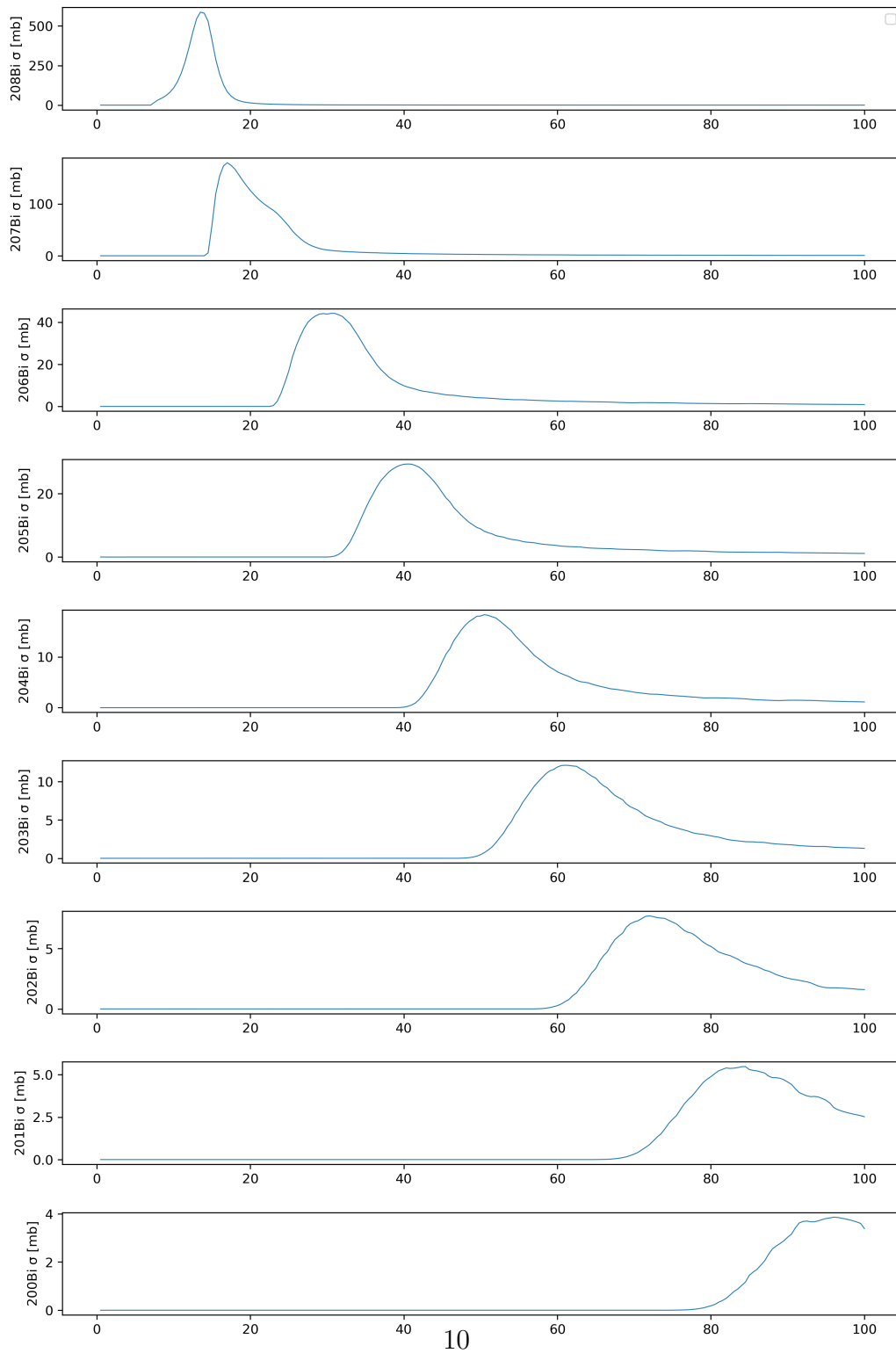


Figure 2.1: The cross-sections obtained via TALYS code used with the level density information outlined above.

Chapter 3

Comparison with the experiment

3.1 Experimental relative yields

The experimental data of saturation activities [2], where the products of $^{209}\text{Bi}(\gamma, \text{xn})$ reactions were obtained by irradiating the bismuth sample with bremsstrahlung of 60, 80 and 100 MeV is used for comparison.

Continuously irradiating bismuth causes saturation in activity. The half-life of the products of photonuclear reactions is long enough such that the irradiated sample can be taken to HPGe detectors to obtain the gamma spectrum. Identifying products with their specific gamma lines and measuring the counts can provide us with the experimental yields of the $^{209}\text{Bi}(\gamma, \text{xn})$ reaction. These yields are calculated relative to ^{206}Bi and are given in (Table 3.1).

These relative yields of the products of $^{209}\text{Bi}(\gamma, \text{xn})$ reactions are to be compared with the ones theoretically calculated using the level density calculations combined with the TALYS cross-section and photon flux simulations.

Since the calculations are relative to one isotope, the comparison with the theoretically obtained values will not suffer from dependence on exact units of photon flux and cross-sections.

isotope	60 MeV	80 MeV	100 MeV
207	-	7.3	6.7
206	1.0	1.0	1.0
205	0.41	0.45	0.45
204	0.163	0.173	0.177
203	0.073	0.087	0.097
202	0.02	0.038	0.046
201	0.0055	0.013	0.02
200	-	0.0025	0.0059

Table 3.1: Experimental relative saturation activities (relative yields).

3.2 Theoretical relative yields

The saturation activity:

$$R = \int_{E_t}^{E_s} \Phi(E)\sigma(E)dE, \quad (3.1)$$

can be calculated knowing the TALYS cross-section $\sigma(E)$, obtained with the use of our level density calculations, and the photon flux $\phi(E)$, modeled in GEANT4. The integral boundaries are the threshold energy for the reaction to occur E_t and the maximum energy of the photon flux E_s . The flux and cross-section are taken with the same binning of 1 [MeV]. The photon flux spectrum was generated using GEANT4 code for bremsstrahlung of 60, 80, and 100 MeV, as these were the energies used in the experiment, and for the geometry matching the one in the experiment. The flux spectrum can be seen in Figure 3.1.

Integrating (3.1) for each of the cross-sections in Figure 2.1, the saturation activities for the corresponding isotopes are obtained and are stated relative to ^{206}Bi saturation activity in Table 3.2. To make further comparisons, another theoretical calculation [2] of relative yields without the use of TALYS is considered.

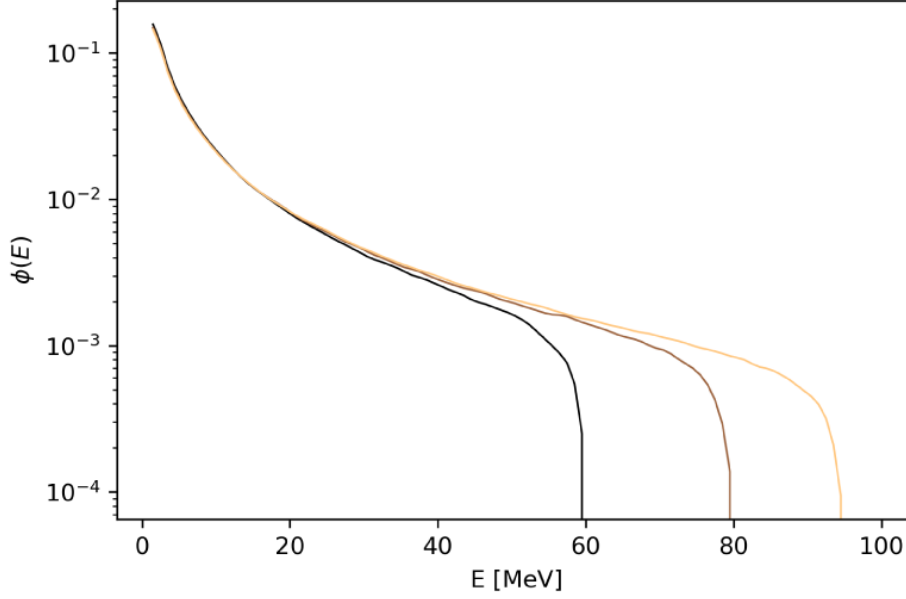


Figure 3.1: Photon flux from GEANT4 simulations of the experiment.

isotope	60 MeV	80 MeV	100 MeV
207	5.53	5.19	5.05
206	1.0	1.0	1.0
205	0.44	0.48	0.49
204	0.15	0.21	0.23
203	0.02	0.11	0.13
202	0.00	0.04	0.06
201	0.00	0.01	0.03
200	0.00	0.0	0.01

Table 3.2: Relative saturation activities (relative yields) calculated using cross-sections from TALYS and photon flux from GEANT4.

3.3 Comparison and conclusions

Finally, the relative yields obtained from the outlined TALYS calculations, from the experiments, and the independent theoretical calculations are labeled 'Calculations with TALYS', 'Experimental', and 'Theoretical calculations' in Figure 3.2, respectively.

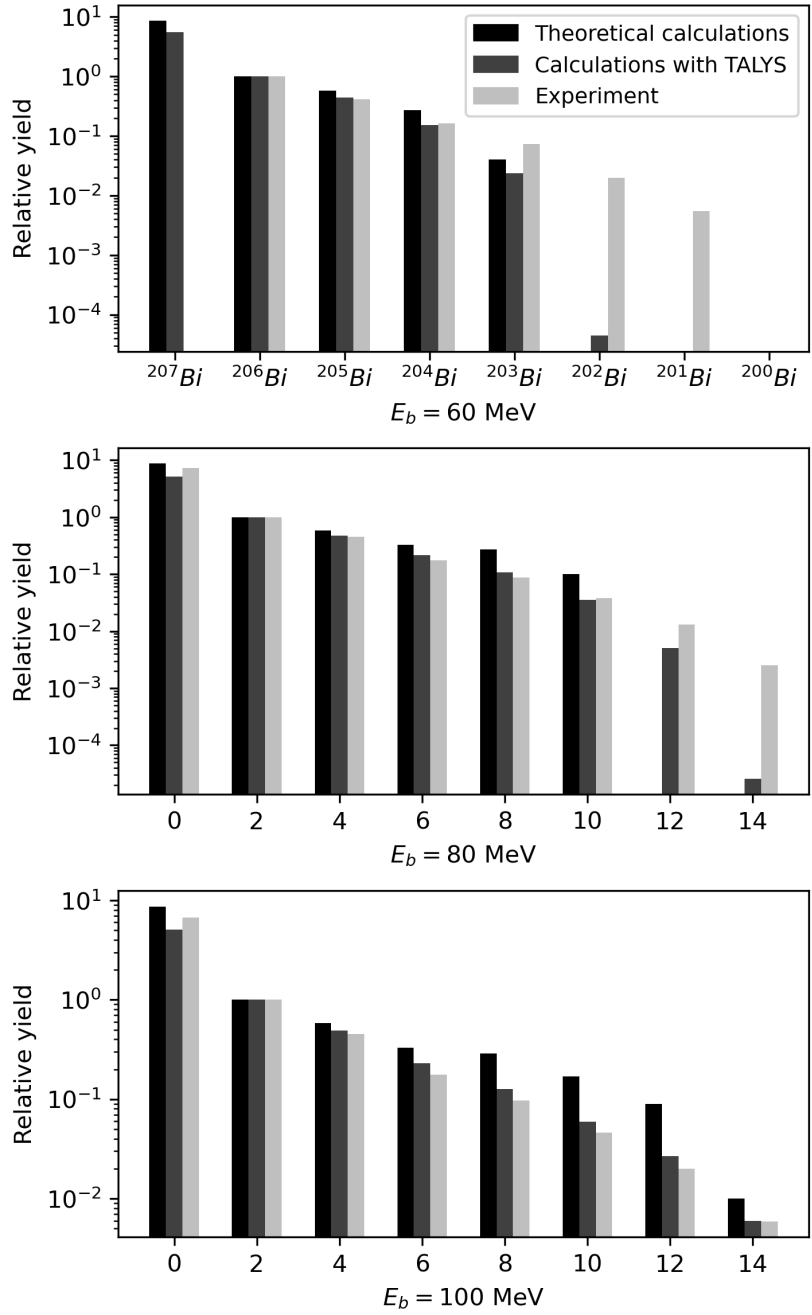


Figure 3.2: Comparison of relative yields obtained from the outlined calculations with TALYS, experimental results, and independent theoretical calculations.

Conclusions

From the results in Figure 3.2, it is noticeable that the experiments don't match the theory at 60 MeV bremsstrahlung energy when more than six neutrons are emitted. The energy of 60 MeV is not sufficient to abundantly produce isotopes with the mass number 202 and less since the separation energy per nucleon is around 7.8 MeV while taking into account that neutrons produced to take on the Maxwellian distribution of energy.

This might indicate the need for further examination of the spectra, such that the source of the experimental yields presented in Figure 3.2 for more than six neutrons emitted are better established.

The gamma spectrum used for the experimental yields had also a noticeable amount of lead, raising the possibility of proton emission effects on calculations. This is to be investigated further by implementing the combinatorial method of counting up the states and using it for the pre-equilibrium reactions.

Bibliography

- [1] P. Decowski et al. “On Superconductivity Effects in Nuclear Level Density”. In: *Nuclear Physics A* 110.2 (1968), pp. 129–141.
- [2] et al Demichev M. “Study of $^{209}\text{Bi}(\gamma, \text{xn})$ Reactions in Energy Region up To 100 MeV”. In: *Physics of Atomic Nuclei* 85.6 (2022).
- [3] W. Greiner and J.A. Maruhn. *Nuclear Models*. Springer-Verlag Berlin Heidelberg, 1996.
- [4] J. R. Huizenga and Moretto L.G. “Nuclear Level Densities”. In: *Annual Review of Nuclear Science* (1972).
- [5] A. Koning, S. Hilaire, and S. Goriely. “TALYS: modeling of nuclear reactions”. In: *The European Physical Journal A* 59 (2023).
- [6] A. Rahmatinejad and T. M. Shneidman. “Collective enhancements in the level densities of Dy and Mo isotopes”. In: *Physical Review C* 101 (2020).
- [7] P. Ring and P. Schuck. *The Nuclear Many-Body Problem*. Springer-Verlag New York, 1980.
- [8] M. Sano and Yamasaki S. “Phase Transition and Level Density of Atomic Nuclei”. In: *Progress of Theoretical Physics* 29.3 (1963).